Unified Analytical Expressions for Calculating Resonant Frequencies, Transimpedances, and Equivalent Input Noise Current Densities of Tuned Optical Receiver Front Ends

Qing Zhong Liu, *Student Member, IEEE*

Abstract—Unified analytical expressions have been derived for calculating the resonant frequencies, transimpedances and equivalent input noise current densities of the four most widely used tuned optical receiver front ends built with FET's and p-i-n diodes. A more accurate FET model has been used to improve the accuracy of the analysis. The Miller's capacitance has been taken into account, and its impact on the performances of the tuned front ends has been demonstrated. The accuracy of the expressions has been verified by Touchstone simulations. The agreement between the calculated and simulated performances of the front ends is very good. The expressions can be used to investigate the performances of different tuned front ends in a very simple way and provide a good starting point for further computer optimizations of the front ends.

I. INTRODUCTION

THE RECEIVER front end is one of the most important circuits in the optical fiber transmission systems, because it essentially determines the sensitivity of the system [1]. The sensitivity of an optical receiver is limited by different noise sources, for example, a signal dependent noise term due to the incident optical power, a noise term due to the photo diode dark current and noise contributions from the receiver pre-amplifier. Among the noise factors in the pre-amplifier, a noise term from the FET channel, which is proportional to the square of the frequency f^2, is a dominating one for high frequency and wideband applications.

In order to suppress the noise contribution from f^2, different tuning networks have been proposed and applied between the photo detector and the preamplifier. As a result, the receiver sensitivity has been improved dramatically in the frequency range of interest. In general, there are four different types tuned front ends which have been used widely: serially, parallel, transformer and mixed tuned front ends [2]. For baseband and coherent homodyne transmission systems, where a low pass char-

acteristic is needed, the serially tuning network should be applied. For coherent heterodyne and subcarrier multiplexing (SCM) systems with bandpass characteristics, one of the other three tuning networks can be utilized. For previous work on the calculation of transimpedances and equivalent input noise current densities of the tuned front ends, the reader is referred to [2]-[5].

In general, to optimize the performance and minimize the sensitivity on component tolerances, computer optimizations are needed before the front ends are built. It is important to provide a good starting point for the optimizations and to avoid the local minima in the final optimizations. It is also helpful to compare the performances of different tuned front ends in a simple and quick way, and to select a suitable configuration of the front ends for a specified application.

In this paper, we will study the performances of the tuned optical receiver front ends in a general context, and present a set of unified analytical and simple expressions, which can be used to calculate the resonant frequencies, transimpedance and equivalent input noise current density of a mixed tuned front end, based on a p-i-n diode and a FET. The expressions can also be applied to the other three configurations of tuned front ends by simple modifications. A few new contributions have been made in the paper. In the derivation of the expressions, the Miller's capacitance, which has been omitted in the previous studies, has been taken into account. In fact, neglecting the Miller's capacitance results in an over-estimation of transimpedance and an underestimation of equivalent input noise current density of the front end. A more accurate model of FET's has been applied in the analysis of the transimpedances and equivalent input noise current densities. This results in a more reliable prediction of the front end performances. The accuracy of the expressions has been verified by using the Touchstone simulator from EESOF. The comparisons between the calculated and simulated front end performances will be presented.

In Section II, we will present the derivation of the analytical expressions for calculating the resonant frequencies, transimpedance and equivalent input noise current density of the mixed tuned optical receiver front end. By

simple modifications, the expressions can be easily applied to the other three configurations of the tuned front ends. In Section III, we will show some numerical results of different tuned front ends and comparisons between the performances calculated by using the analytical expressions and simulated by using Touchstone simulator. In Section IV conclusions are given.

II. DERIVATION OF THE ANALYTICAL EXPRESSIONS

The diagram of a general tuned optical receiver front end based on a p-i-n diode and a FET is shown in Fig. 1. The pin diode is modelled as a current source I_s, a junction capacitance C_j, and a series resistance R_j. The FET is represented by a well-known equivalent circuit model, which is valid for both MESFET's and HEMT's. Since drain resistance R_d is much smaller than either channel resistance R_{ds} or load resistance R_L, its influence can be neglected. In general, the value of capacitance C_{ds} is smaller than either C_{gs} or C_{gd}, therefore, C_{ds} can also be neglected in the analysis. The tuning network can be selected according to different applications. The four different tuning networks, which have been used widely, are shown in Fig. 2. The mixed tuning network shown in Fig. 2 (d) is selected for the present study. In the mixed tuning network, there are three inductances L_s, L_{p1}, and L_{p2}, which are used to tune the front end performances. The front end amplifier is assumed to be terminated by a 50 Ω load in the following analysis.

To derive the expressions for the resonant frequencies of the front end, we assume that resistances R_g, R_{in}, and R_s can be neglected, because these resistances will only influence the amplitude of the resonant peaks. For the first order approximation, the source inductance l_s is also omitted. Assuming that, we can show that the transfer function from the photo diode to the gate source capacitance C_{gs} is given by
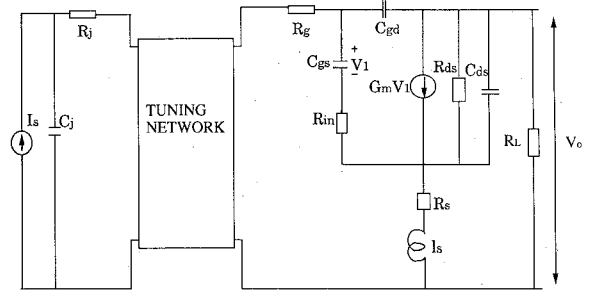

Fig. 1. Diagram of a general tuned optical receiver front end.

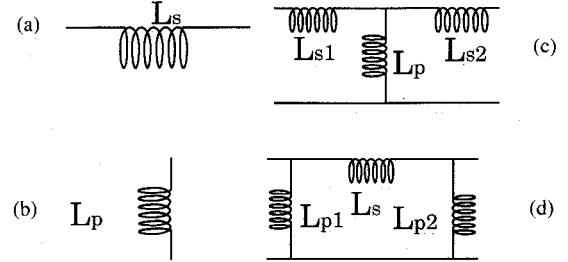
Fig. 2. (a) Serially tuning network. (b) Parallel tuning network. (c) Transformer tuning network. (d) Mixed tuning network.

itance to the performances of tuned front ends will be demonstrated in Section III.

From the tuning network of the mixed front end, we can see that there are two resonant frequencies due to the combination of the network, the diode and the FET. Equating the denominator of (1) to zero, we have

$$A\omega^4 + B\omega^2 + C = 0 \tag{2}$$

where the coefficients A, B and C are given by

$$A = L_s L_{p1} L_{p2}$$

$$Z_t = \frac{V_1}{I_s} = \frac{Z_a Z_b Z_{p1} Z_{p2}}{[Z_b Z_{p2} + Z_s(Z_{p2} + Z_b)](Z_{p1} + Z_a) + (Z_{p2} + Z_b)Z_1 Z_{p1}} \tag{1}$$

where

$$Z_a = \frac{1}{j\omega C_j}$$

$$Z_b = \frac{1}{j\omega(C_{gs} + C'_{gd})}$$

$$Z_{p1} = j\omega L_{p1}$$

$$Z_{p2} = j\omega L_{p2}$$

$$Z_s = j\omega L_s$$

$$C'_{gd} = [1 + g_m(R_{ds} \| R_L)]C_{gd}.$$

The term C'_{gd} in the above expressions represents the so called Miller's capacitance, and the impact of the capac-

$$B = -\left[L_{p1} L_{p2}\left(\frac{1}{C_j} + \frac{1}{C_{gs} + C'_{gd}}\right) \right.$$
$$\left. + \frac{L_{p1} L_s}{C_{gs} + C'_{gd}} + \frac{L_{p2} L_s}{C_j} \right]$$

$$C = \frac{L_s}{C_j(C_{gs} + C'_{gd})}$$

By solving the (2) with the condition that the resonant frequencies are greater than zero, we obtain the expressions for the two resonant frequencies of the mixed tuned

front end:

$$F_1 = \frac{1}{2\pi} \left[\frac{-B + \sqrt{B^2 - 4AC}}{2A} \right]^{1/2} \quad (3)$$

$$F_2 = \frac{1}{2\pi} \left[\frac{-B - \sqrt{B^2 - 4AC}}{2A} \right]^{1/2}. \quad (4)$$

For calculation of the transimpedance, the resistances R_g, R_{in}, and R_s are taken into account. The source inductance is also included. To derive the expression for the trans-impedance of the tuned front end, we calculate the voltage V_1 on gate source capacitance C_{gs} as a function of input current I_s. Secondly, the output voltage V_0 of the front end amplifier is determined. Finally, the transimpedance is obtained by dividing the V_0 by I_s. Following the above mentioned steps, we derived the following expression for the transimpedance:

where

$$Z_{21} = \frac{Z_a Z_2 Z_{gs} Z_{em}}{Z_1 Z_3 [(1 + g_m Z_{gs}) Z_{ss} + Z_{in} + Z_{gs} + Z_{em}]}$$

$$Z_{GO} = Z_{gs} \| (Z_{em} + Z_{ss} + Z_{in})$$

$$A = \frac{Z_{ss} + Z_{in} + Z_{gs} + Z_{em}}{(1 + g_m Z_{gs}) Z_{ss} + Z_{in} + Z_{gs} + Z_{em}}$$

The parameters P, R, and C_{or} in expression (6) are drain noise coefficient, gate noise coefficient and correlation coefficient between the drain and gate noises. P and R depend on the bias conditions and technological parameters of the devices used. The parameter C_{or} is mainly determined by the device parameters [7].

$$Z_{tm} = \frac{-g_m R_{ds} R_L Z_{gs} Z_a Z_2 Z_4}{[Z_{em} + Z_{gs} + Z_{in} + Z_{ss}(1 + g_m Z_{gs})][R_{ds} + R_L + Z_{ss}](Z_3 + Z_4)Z_1} \quad (5)$$

where

$$Z_{ss} = j\omega l_s + R_s$$

$$Z_{gs} = \frac{1}{j\omega C_{gs}}$$

$$Z_{in} = R_g + R_{in}$$

$$Z'_{gd} = \frac{1}{j\omega C'_{gd}}$$

$$Z_1 = Z_a + R_j$$

$$Z_2 = Z_1 \| Z_{p1}$$

$$Z_3 = Z_2 + Z_s$$

$$Z_4 = Z_{p2} \| Z'_{gd}$$

$$Z_{em} = Z_3 \| Z_4.$$

In [6], an analytical expression was given for calculating the equivalent input noise current density of a transformer tuned front end. Based on that work, we derived an expression for determining the noise current density of the mixed tuned front end. Since we are interested in the optical receiver front ends for wideband application, only the FET's channel noises are considered. For a complete analysis, the noise contributions from the resistances R_g and R_j should be taken into account. The impact of R_g and R_j to the total noise performances of the front ends have been reported in [4] and [6]. It should be mentioned that the Miller's capacitance has been included in the present study. It can be shown that the equivalent input noise current density of the mixed tuned front end can be approximated as

$$\frac{\overline{i^2}}{\Delta f} = \frac{4KT}{gm} \frac{1}{|Z_{21}/A|^2} \{ P + R|Z_{GO}|^2 (\omega C_{gs})^2$$

$$- 2C_{or} \sqrt{PR} (\omega C_{gs} \, \mathrm{Im} \, [Z_{GO}]) \} \quad (6)$$

All the expressions derived above can be easily applied to the other three front end configurations. To obtain the expression for calculating resonant frequency of a serially tuned front end, we assume that the values of parallel inductances L_{p1} and L_{p2} are infinite. It can be easily verified that F_1 is the resonant frequency of the serially tuned front end. To calculate the transimpedance and equivalent input noise current density, Z_{p1} is set to be infinite, and Z_{p2} is replaced by a load resistance R_b. A noise term $4KT/R_b$ resulting from the load resistance R_b has to be added in the calculation of the noise current density.

The expressions for a parallel tuned front end are obtained by letting L_s be infinitesimal. It can also be verified that F_2 is the resonant frequency of the front end. To calculate the transimpedance and equivalent input noise current density, we simply let Z_s be zero.

For the transformer tuned front end, there are also three inductances in the tuning network as shown in Fig. 2 (c). By using the well known π to T network transformation, the two resonant frequencies, transimpedance, and equivalent input noise current density of the transformer tuned front end can also be calculated by using the expressions (3)–(6).

III. NUMERICAL RESULTS AND COMPARISONS

To demonstrate the accuracy of the expressions, the transimpedances and equivalent input noise current densities of the tuned front ends have been calculated by using the expressions derived above and simulated by using Touchstone simulator. Since the resonant frequencies of the front ends cannot be simulated directly by means of the Touchstone simulator, the accuracy of the expressions will be verified indirectly by comparing the resonant frequencies calculated by means of (3) and (4) with the frequencies where the transimpedance peaks occur. Since the investigations of the tuned front ends are carried out in a

TABLE I
THE VALUES OF THE PARAMETERS IN
THE EQUIVALENT CIRCUIT OF THE
HEMT PRE-AMPLIFIER

C_{gs} (pf)	0.20
C_{gd} (pf)	0.02
C_{ds} (ff)	7.20
g_m (ms)	45.0
R_{in} (Ω)	4.1
R_{ds} (Ω)	200
R_s (Ω)	3.5
R_g (Ω)	2.0
R_L (Ω)	200
l_s (nH)	0.5

general context, no optimizations of the performances of the front ends have been made. To design a front end for a specified application, further computer simulations and optimizations are needed.

The photo diode used is a p-i-n diode from BT&D (PDC 4300) with C_j of 0.12 pF and R_j of 10.0 Ω [8]. The FET is a HEMT from NEC (NE20200). The performances of the front ends have been simulated, based on the model of the diode and S-parameters of the HEMT provided by the manufacturer. The values of the parameters in the equivalent circuit of the HEMT shown in Fig. 1 are listed in Table I.

Fig. 3 shows the resonant frequencies of a serially and a parallel tuned front end as functions of tuning inductances. For both front ends, the tuning range of the resonant frequencies is very large when the values of the tuning inductances are small. A significant difference between the two tuned front ends is that the resonant frequencies are different for the same value of tuning inductances. The resonant frequency of the serially tuned front end is much higher than that of the parallel tuned front end. With the tuning inductance of 2.0 nH, the resonant frequencies of the serially and parallel tuned front ends are 12.5 GHz and 5.9 GHz, respectively.

For the transformer and mixed tuned front ends, there are two resonant frequencies due to the combination of the tuning network, the photo diode and the HEMT. In the following discussions, F_1 and F_2 are defined as the higher and lower resonant frequencies, respectively. The sensitivity of the resonant frequencies to the inductances is different as will be shown in the following. In Fig. 4 (a) and (b), the resonant frequencies F_1 and F_2 of the transformer tuned front end are shown as function of tuning inductances, respectively. Comparing the tuning characteristics of the different inductances, we can see that the most efficient way to tune F_1 is to change the value of serial inductance L_{s1}. By increasing the value of L_{s1} from 1.0 nH to 10.0 nH, F_1 can be tuned from 7.7 GHz to 4.4 GHz. On the other hand, F_1 is not sensitive to the variation of the parallel inductance L_p. F_1 is only decreased by 0.4 GHz when L_p is varied in the same range. Similarly we can determine the inductance which has a significant influence on the lower resonant frequency F_2. It has been observed that a large tuning range of F_2 is obtained by
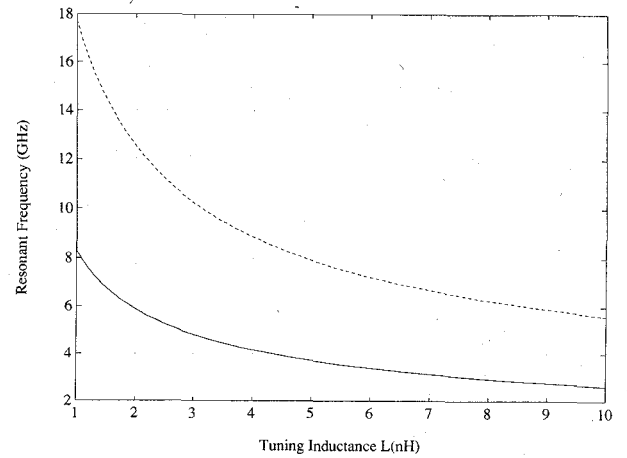

Fig. 3. Resonant frequencies of the serially and parallel tuned front ends as function of tuning inductances. Dashed line: resonant frequency of the serially tuned front end. Solid line: resonant frequency of the parallel tuned front end.
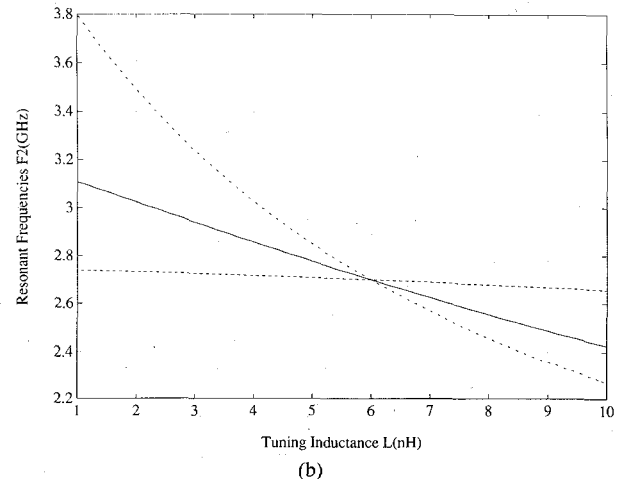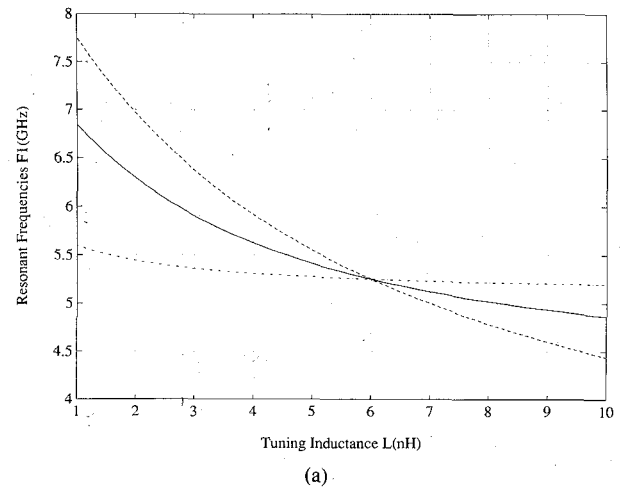

(a)

(b)

Fig. 4. (a) Resonant frequency F_1 of the transformer tuned front end as function of tuning inductances. Dashed line: F_1 as function of serially tuning inductance L_{s1} with $L_{s2} = L_p = 6.0$ nH. Solid line: F_1 as function of serially tuning inductance L_{s2} with $L_{s1} = L_p = 6.0$ nH. Dashdot line: F_1 as function of parallel tuning inductance L_p with $L_{s1} = L_{s2} = 6.0$ nH. (b) Resonant frequency F_2 of the transformer tuned front end as function of tuning inductances. Dashed line: F_2 as function of serially tuning inductance L_{s1} with $L_{s2} = L_p = 6.0$ nH. Solid line: F_2 as function of serially tuning inductance L_{s2} with $L_{s1} = L_p = 6.0$ nH. Dashdot line: F_2 as function of parallel tuning inductance L_p with $L_{s1} = L_{s2} = 6.0$ nH.

changing the value of the parallel inductance L_p. F_2 is nearly independent of the variation of serial tuning inductance L_{s1}.

In Fig. 5 (a) and (b), the resonant frequencies F_1 and F_2 of the mixed tuned front end are shown as function of tuning inductances, respectively. The higher resonant frequency F_1 is most sensitive to the variation of the serial inductance L_s. The tuning range of more than 10 GHz can be obtained by increasing L_s from 1.0 nH to 10.0 nH. By varying the parallel inductance L_{p2} in the same range, however, F_1 is only tuned by 2.5 GHz. For the lower resonant frequency, we found that the most efficient way to tune F_2 is to change the value of the parallel inductance L_{p2}. By increasing the L_{p2} from 1.0 nH to 10.0 nH, F_2 is decreased from 7.7 GHz to 4.1 GHz. On the other hand, the changes of serial inductance L_s have a very small impact on F_2. The deviation of F_2 is only about 0.2 GHz for the same variation of L_s. These facts indicate that the tuning inductances have different influences on the resonant frequencies. They can be selected and controlled to obtain the required bandwidth of the front ends.

In Fig. 6 (a)–(d), the comparisons between the calculated and simulated transimpedances of the four tuned front ends are shown. For the serially tuned front end shown in Fig. 6 (a), the transimpedance is about 45 dBΩ from dc to 7.0 GHz when the value of the serial tuning inductance is 6.0 nH. The agreement between the simulated and calculated results is good. At lower frequency, the deviation between the results is slightly large, and the calculated transimpedance is about 2.5 dB higher than the simulated one. For the parallel tuned front end shown in Fig. 6 (b), the maximum deviation between the simulated and calculated transimpedances is less than 2.0 dB in the bandwidth from 1.0 GHz to 8.0 GHz. It can be also seen that the transimpedance of the parallel tuned front end is higher than 50 dBΩ in the bandwidth of 1.3 GHz. Therefore the parallel tuned front end is only useful for some narrow band applications, because the transimpedance is reduced rapidly as the frequency is deviated from the resonant frequency. In order to increase the working bandwidth either the transformer or mixed tuned front ends have to be applied. In Fig. 6 (c), the comparison between the calculated and simulated transimpedances of the transformer tuned front end is shown. The agreement between the simulated and calculated performances is also good. The transimpedance of the transformer tuned front end is higher than 50 dBΩ in a bandwidth of about 3.3 GHz. In the case of mixed tuned front end shown in Fig. 6 (d), the agreement between the calculated and simulated transimpedances is very good, and the maximum deviation between the simulated and calculated results is less than 2.0 dB in the frequency range of 1.0 GHz to 10.0 GHz. The transimpedance of the mixed tuned front end is higher than 45 dBΩ in the bandwidth of 5.0 GHz. Comparing the transformer and mixed tuned front ends with same values of tuning inductances, we found that the mixed tuned front end is more suitable for the applications where high operating frequency and large bandwidth are needed.
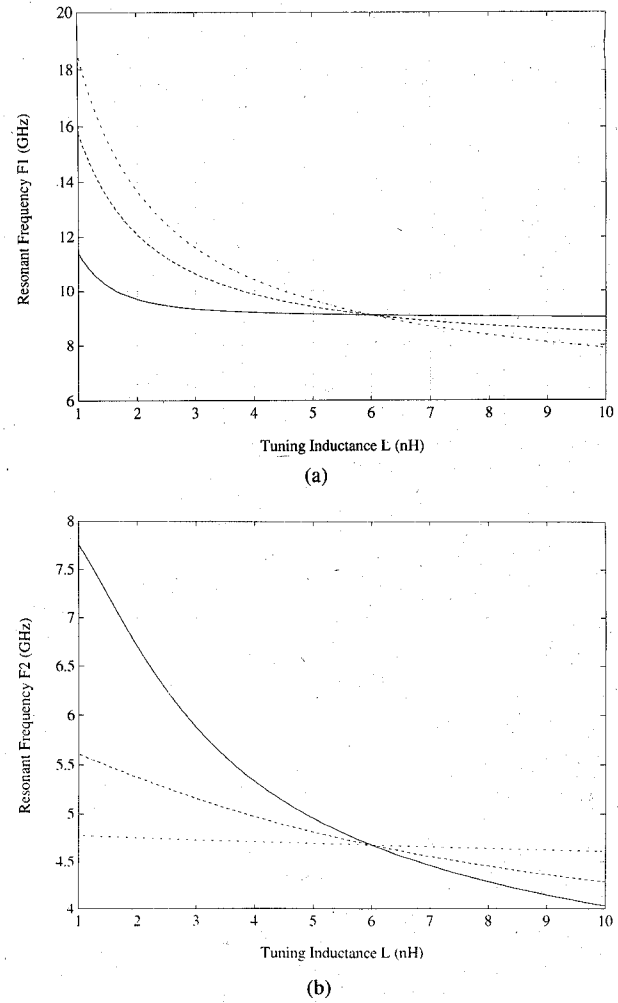

(a)

(b)

Fig. 5. (a) Resonant frequency F_1 of the mixed tuned front end as function of tuning inductances. Dashed line: F_1 as function of parallel tuning inductance L_{p1} with $L_{p2} = L_s = 6.0$ nH. Solid line: F_1 as function of parallel tuning inductance L_{p2} with $L_{p1} = L_s = 6.0$ nH. Dashdot line: F_1 as function of serially tuning inductance L_s with $L_{p1} = L_{p2} = 6.0$ nH. (b) Resonant frequency F_2 of the mixed tuned front end as function of tuning inductances. Dashed line: F_2 as function of parallel tuning inductance L_{p1} with $L_{p2} = L_s = 6.0$ nH. Solid line: F_2 as function of parallel tuning inductance L_{p2} with $L_{p1} = L_s = 6.0$ nH. Dashdot line: F_2 as function of serially tuning inductance L_s with $L_{p1} = L_{p2} = 6.0$ nH.

To verify the accuracy of the expressions (3) and (4), we compare the resonant frequencies calculated by using (3) and (4) with frequencies where the peaks in the simulated and calculated transimpedances occur. The results are summarized in Table II. The resonant frequencies calculated by using expression (3) and (4) are listed in column A. In column B, the frequencies, which correspond to the peaks of the simulated transimpedances of the front ends, are shown. The frequencies, where the peaks of the transimpedances calculated by using expression (5) occur, are listed in column C. Comparing the resonant frequencies obtained by different methods, we can see that the expressions (3) and (4) can be used to predict the resonant frequencies of the front ends and reasonable accurate results have been obtained.

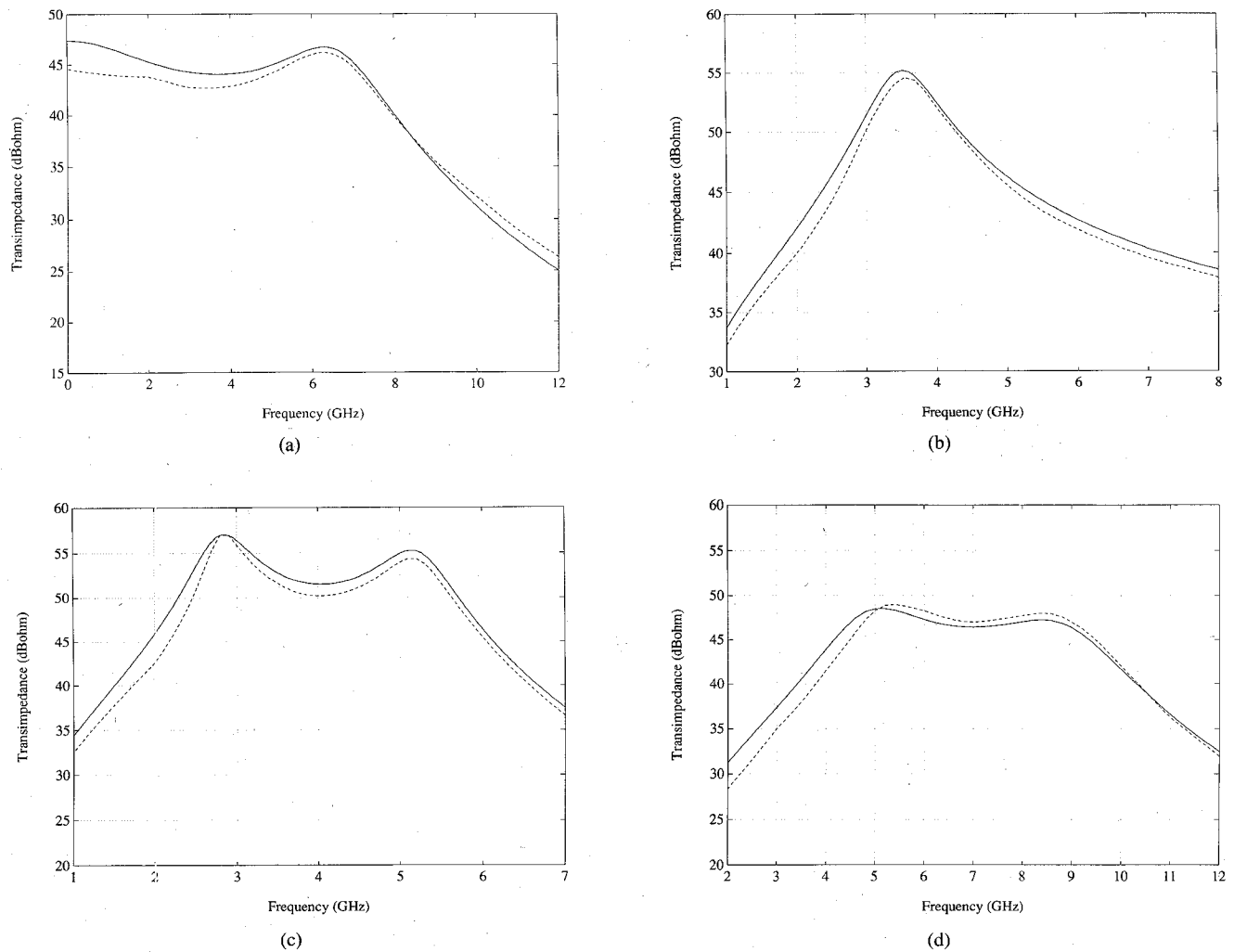In Fig. 7 (a)–(d), the comparisons between the calculated and simulated equivalent input noise current densi-

Fig. 6. (a) Comparison between the calculated and simulated transimpedances of the serially tuned front end. Solid line: calculated result. Dashed line: simulated result. L_s = 6.0 nH, R_b = 200 Ω. (b) Comparison between the calculated and simulated transimpedances of the parallel tuned front end. Solid line: calculated result. Dashed line: simulated result. L_p = 6.0 nH. (c) Comparison between the calculated and simulated transimpedances of the transformer tuned front end. Solid line: calculated result. Dashed line: simulated result. $L_p = L_{s1} = L_{s2}$ = 6.0 nH. (d) Comparison between the calculated and simulated transimpedances of the mixed tuned front end. Solid line: calculated result. Dashed line: simulated result. $L_{p1} = L_{p2} = L_s$ = 6.0 nH.

TABLE II
THE COMPARISON BETWEEN THE CALCULATED AND SIMULATED RESONANT
FREQUENCIES OF THE FOUR TUNED FRONT ENDS

	A	B	C	
F_s (GHz)	7.22	6.36	6.36	L_s = 6.0 nH
F_p (GHz)	3.39	3.58	3.54	L_p = 6.0 nH
F_{t1} (GHz)	5.25	5.15	5.15	$L_{s1} = L_{s2} = L_p$ = 6.0 nH
F_{t2} (GHz)	2.88	2.85	2.85	$L_{s1} = L_{s2} = L_p$ = 6.0 nH
F_{m1} (GHz)	9.17	8.65	8.53	$L_{p1} = L_{p2} = L_s$ = 6.0 nH
F_{m2} (GHz)	4.67	5.35	5.10	$L_{p1} = L_{p2} = L_s$ = 6.0 nH

F_s: resonant frequency of the serially tuned front end.
F_p: resonant frequency of the parallel tuned front end.
F_{t1}: high resonant frequency of the transformer tuned front end.
F_{t2}: low resonant frequency of the transformer tuned front end.
F_{m1}: high resonant frequency of the mixed tuned front end.
F_{m2}: low resonant frequency of the mixed tuned front end.

ties of different tuned front ends are shown. For the serially tuned front end shown in Fig. 7 (a), the agreement between the calculated and simulated equivalent input noise current densities is very good. The maximum deviation between the calculated and simulated results is less than 2.0 pA/√Hz. The noise current density is less than 10.0 pA/√Hz in the frequency range of dc to 8.5 GHz. The minimum noise current density calculated is about 5.0 pA/√Hz. The comparison between the calculated and simulated equivalent input noise current densities of the parallel tuned front end is shown in Fig. 7 (b). A good agreement has been obtained between the calculated and simulated equivalent input noise current densities. The maximum deviation between the calculated and the simulated results is less than 2.0 pA/√Hz from 1.0 GHz to 7.0 GHz. Even though a flat transimpedance of the parallel tuned front end is obtained only in a relatively nar-
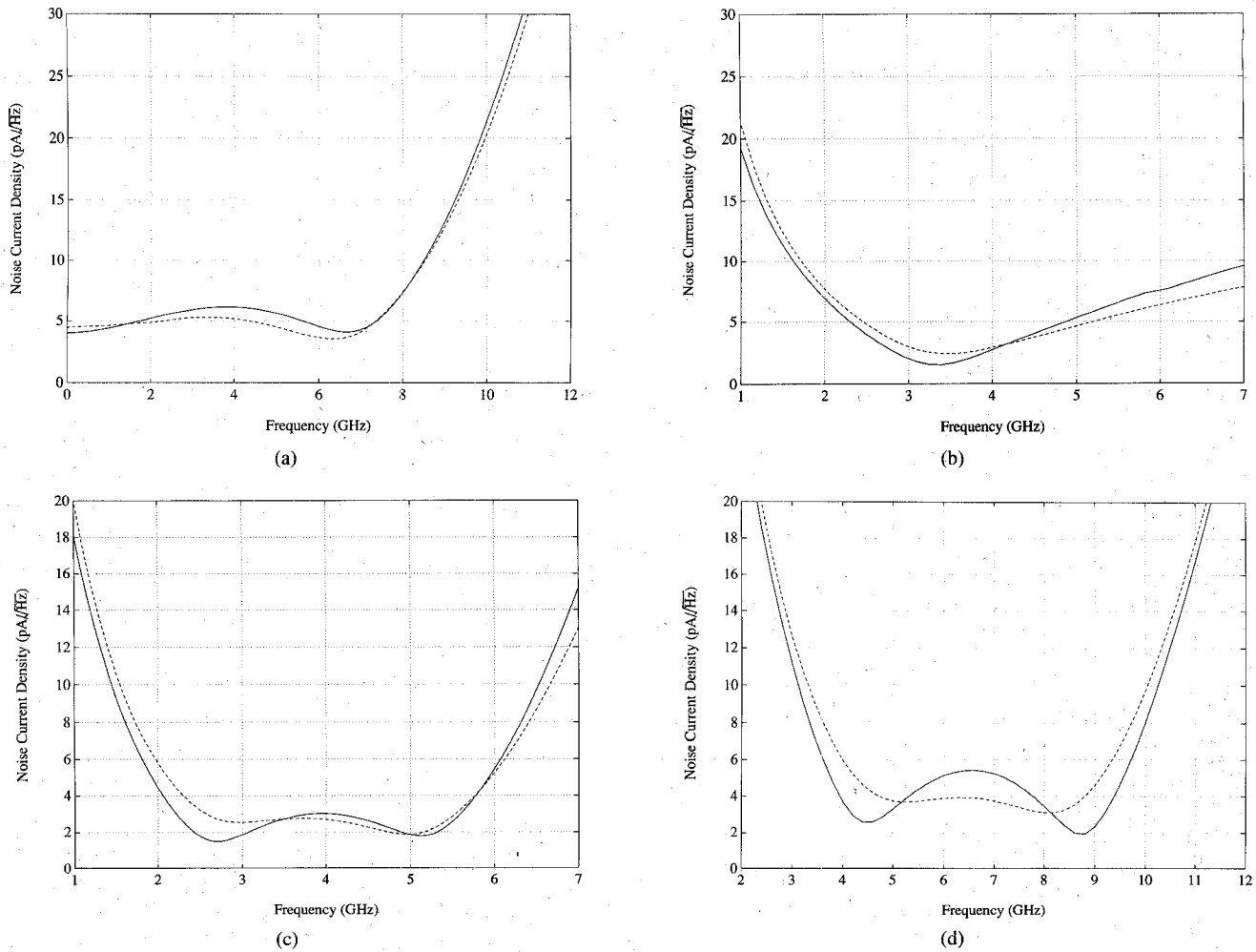
Fig. 7. (a) Comparison between the calculated and simulated equivalent input noise current densities of the serially tuned front end. Solid line: calculated result. Dashed line: simulated result. L_s = 6.0 nH, R_b = 1000 Ω. (b) Comparison between the calculated and simulated equivalent input noise current densities of the parallel tuned front end. Solid line: calculated result. Dashed line: simulated result. L_p = 6.0 nH. (c) Comparison between the calculated and simulated equivalent input noise current densities of the transformer tuned front end. Solid line: calculated result. Dashed line: simulated result. $L_p = L_{s1} = L_{s2} = 6.0$ nH. (d) Comparison between the calculated and simulated equivalent input noise current densities of the mixed tuned front end. Solid line: calculated result. Dashed line: simulated result. $L_{p1} = L_{p2} = L_s = 6.0$ nH.

row bandwidth, the noise current density can be low in a wide bandwidth. The noise current density is less than 10.0 pA/√Hz in the frequency range from 1.7 GHz to 7.0 GHz and the minimum noise current density calculated is about 2.0 pA/√Hz. Fig. 7 (c) shows the comparison between the calculated and simulated equivalent input noise current densities of the transformer tuned front end. In the frequency range of 1.5 GHz to 6.3 GHz, which is the required bandwidth for some SCM transmission system [9], the equivalent input noise current density of the transformer tuned front end is less than 10.0 pA/√Hz. The minimum noise current density calculated is less than 2.0 pA/√Hz. The agreement between the calculated and simulated performances is good in the bandwidth of interest. In Fig. 7 (d), the comparison between the calculated and simulated equivalent input noise current densities of the mixed tuned front end is shown. A good agreement has been obtained between the calculated and the simulated equivalent input noise current densities

in the frequency range from 2.0 GHz to 11.0 GHz. The maximum deviation between the calculated and simulated results is less than 2.0 pA/√Hz. The calculated noise current density is less than 10.0 pA/√Hz in the frequency range from 3.2 GHz to 10.2 GHz. The minimum noise current density calculated is about 3.0 pA/√Hz.

Finally we show the effect of the Miller's capacitance on the performances of the tuned front ends. The Miller's capacitance has been omitted in the calculation of the equivalent input noise current density of the front ends [10]–[11]. Based on the present study, we found that neglecting the Miller's capacitance results in an over-estimation of transimpedances and an underestimation of equivalent input noise current densities of the front ends. Since the Miller's capacitance is proportional to the gate drain capacitance C_{gd}, we can investigate the impact of C_{gd} on the front ends performances. In Figs. 8 (a) and (b), the transimpedances and equivalent input noise current densities of a mixed tuned front end are shown with C_{gd}
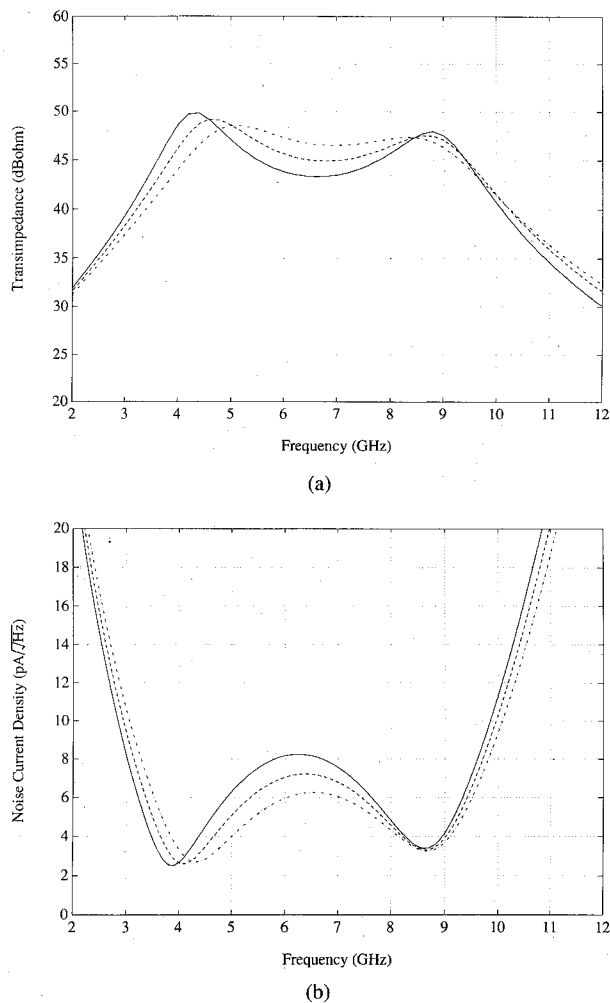
(a)

(b)

Fig. 8. (a) Transimpedances of the mixed tuned front end with gate drain capacitance C_{gd} as parameters. Dashdot line: $C_{gd} = 0.02$ pF. Dashed line: $C_{gd} = 0.04$ pF. Solid line: $C_{gd} = 0.06$ pF. $L_{p1} = L_{p2} = L_s = 6.0$ nH. (b) Equivalent input noise current densities of the mixed tuned front end with gate drain capacitance C_{gd} as parameters. Dashdot line: $C_{gd} = 0.02$ pF. Dashed line: $C_{gd} = 0.04$ pF. Solid line: $C_{gd} = 0.06$ pF. $L_{p1} = L_{p2} = L_s = 6.0$ nH.

as a parameters, respectively. It can be clearly seen that the transimpedance is reduced and the equivalent input noise current density is increased when the value of C_{gd} is increased. A 3.0 dB reduction of transimpedance and 2.0 pA/$\sqrt{Hz}$ increase of the equivalent input noise current density have been observed when the values of C_{gd} is increased from 0.02 pF to 0.06 pF, respectively.

IV. CONCLUSION

In this paper, we presented a set of unified and analytical expressions for calculating the resonant frequencies, transimpedances and equivalent input noise current densities of the four most widely used tuned optical receiver front ends, based on p-i-n diodes and MESFET's or HEMT's. The accuracy of the analysis has been improved by using a more accurate model of FET's and by taking the Miller's capacitance into account. The performances of the tuned front ends have been studied by using the

expressions derived. The impact of the Miller's capacitance has been illustrated. Neglecting the Miller's capacitance results in an over-estimation of transimpedance and an underestimation of equivalent input noise current density of the front ends. The tuning inductances in the transformer and the mixed tuned front ends have been shown to have different influences on the front ends performances. The performances of the four different tuned front ends have been calculated by using the expression derived and simulated by using microwave simulator Touchstone. Good agreement between the calculated and simulated performances of the front ends has been obtained. The maximum deviation between the calculated and simulated transimpedances and equivalent input noise current densities of the front ends are less than 2.5 dB and 3.0 pA/$\sqrt{Hz}$, respectively. The expressions can be applied for providing a good starting point for further computer optimizations of the front ends. The expressions will find wide applications in predicting performances of tuned optical receiver front ends built with a p-i-n diode and MESFET's or HEMT's for both digital and SCM transmission systems.

ACKNOWLEDGMENT

REFERENCES

[1] S. D. Personick, "Receiver design for digital fibre optic communication," *Bell Syst. Techn. J.*, vol. 52, no. 6, pp. 843–886, 1973.
[2] G. Jacobsen, K. X. Kan, and I. Garrett, "Tuned front end design for heterodyne optical receivers," *J. Lightwave Technol.* vol. 7, no. 1, pp. 105–114, Jan. 1989.
[3] N. Ohkawa, "Fibre optic multigigabit GaAs MIC front end circuit with inductor peaking." *J. Lightwave Technol.* vol. 6, no. 11, pp. 1665–1671, Nov. 1988.
[4] T. E. Darcie, B. L. Kasper, J. R. Talman, and C. A. Burrus, Jr., "Resonant pin-FET receivers for Lightwave subcarrier systems," *J. Lightwave Technol.* vol. 6, no. 4, pp. 582–589, Apr. 1988.
[5] J. Gimlett, "Ultrawide bandwidth optical receivers," *J. Lightwave Technol.* vol. 7, no. 10, pp. 1432–11437, Oct. 1989.
[6] K. E. Alameh, and R. A. Minasian, "Tuned optical receivers for microwave subcarrier multiplexed lightwave systems," *IEEE Trans. Microwave Theory Tech.*, vol. 38, no. 5, pp. 546–551, May 1990.
[7] A. Cappy, "Noise modeling and measurement techniques," *IEEE Trans. Microwave Theory Tech.*, vol. 36, no. 1, pp. 1–10, Jan. 1988.
[8] D. Wake, R. H. Walling, and I. D. Henning, "Planar junction, top illuminated GaAs/InP pin photodiode with bandwidth of 25 GHz," *Electron. Lett.*, vol. 25, no. 15, pp. 967–969, July 1989.
[9] R. Olshansky and V. Lanzisera, "Subcarrier passive optical network for low cost video distribution," in *Proc. Opt. Fibre Communications Conf.* 1989. p. 57.
[10] H. Kressel, *Semiconductor Devices for Optical Communications.* Berlin: Springer, 1980, ch. 4.
[11] E. E. Bert Basch, *Optical fibre transmissions.* Indianapolis, IN: Howard W. Sams, 1987, ch. 12.

Qing Zhong Liu (S'90) was born in Tian Jin, China, on Nov. 12, 1958. He received the B.S. degree in physics from the National Nan Kai University, China, in 1982, and M.S. and Ph.D degrees in electrical engineering from the Technical University of Denmark, in 1988 and 1991, respectively.

From 1982 to 1985, he was with the Shijiazhuang Communications Laboratory, China, where he worked in the analysis and design of microwave transistor oscillators and phase lock loops. From September 1985 to August 1991, he was with the Electromagnetics Institute, Technical University of Denmark. While there, he was involved in the design of dielectric resonator stabilized oscillators, characterization of MESFET's and HEMT's, design of a 10 Gbit/s 2:1 time division multiplexer, modulation of high speed laser diodes, and analysis and design of low noise and wide band optical receiver front ends. Since September 1991 he has been a Postdoctoral Fellow at the University of British Columbia, Canada. His current research interests include modeling and characterization of MESFET's, HEMT's, and HBT's, and their applications to the analysis and design of high speed and low noise circuits for optical fibre communication systems.